

DETC2016-59290

## FORWARD AND INVERSE POSITION KINEMATICS FOR THE RRSSR PARALLEL ROBOT WITH HARDWARE VALIDATION

**Robert L. Williams II, Ph.D.**

Mechanical Engineering Department  
Ohio University  
Athens, Ohio, USA  
[williar4@ohio.edu](mailto:williar4@ohio.edu)

**Ryan Lucas**

Mechanical Engineering Department  
Ohio University  
Athens, Ohio, USA  
[r1133112@ohio.edu](mailto:r1133112@ohio.edu)

**J. Jim Zhu, Ph.D.**

Electrical Engineering  
Ohio University  
Athens, Ohio, USA  
[zhuj@ohio.edu](mailto:zhuj@ohio.edu)

### ABSTRACT

This paper presents forward and inverse position kinematics equations and analytical solutions for the 2-dof RRSSR Parallel Robot. Two ground-mounted perpendicular offset revolute (R) joints are actuated via servomotors, and the single-loop parallel robot consists of passive R-S-S (revolute-spherical-spherical) joints in between the active joints. A study of the multiple solutions in each case is presented, including means to select the appropriate solutions. This rigid-link parallel robot forms the hip joints of the Ohio University RoboCat walking quadruped. The methods of this paper are suitable to assist in design, simulation, control, and gait selection for the quadruped. RoboCat hardware has been built and used to help validate the examples and results of this paper.

### KEYWORDS

RRSSR parallel robot, walking robot, quadruped, RoboCat, forward and inverse kinematics, analytical solutions, multiple solutions, hardware validation.

### 1. INTRODUCTION

Spatial mechanisms and parallel robots with active and passive revolute (R) and spherical joints (S) have been of interest in industry and academia for a long time (e.g. [1]).

The specific RRSSR parallel robot has only been addressed by a few authors. Mooring et al. [2] use a RRSSR parallel robot as an example in their book; however, they simply

calculate the number of degrees-of-freedom (2) and determine the number of kinematic parameters required to specify the robot model (18). They do not present any position or other kinematics analysis equations nor solutions. Simionescu et al. [3] present kinematic analysis for an Ackermann steering mechanism, a spatial RSSR mechanism – this is extended to an RRSSR to model the variable position and orientation of the ground joints. They present a detailed kinematic analysis of the RRSSR device with regard to steering linkage design and performance. However, all of their solutions are obtained numerically, rather than analytically. Earlier [4] and later [5] publications by Simionescu's team again use the RRSSR as an example, again without analytical position kinematics equations solutions. Li and Dai [6] use the RRSSR as an example in their study of metamorphic mechanisms. However, the 2 RR joints are parallel, rather than perpendicular as in the former cases. Further, they do not present detailed kinematic analysis.

Ohio University has developed a walking quadruped robot, the RoboCat (for Robotic Bobcat). The four hip joints are each 2-dof RRSSR parallel robots. The purpose of the current paper is to present detailed position kinematics modeling and analysis for the RRSSR. Analytical solutions are presented for the forward and inverse position kinematics problems. Multiple solutions are considered and a means provided to choose the appropriate solutions automatically. Examples are presented to compare MATLAB simulation vs. hardware results.

## 2. RRSSR PARALLEL ROBOT DESCRIPTION

Figure 1a shows a photograph of the original RoboCat walking quadruped robot designed and built at Ohio University, with 1-dof flexion/extension hips. Figure 1b shows a photograph of the RoboCat with improved legs, changing to 2-dof flexion/extension and abduction/adduction hips.



Figure 1a. Original RoboCat Walking Quadruped



Figure 1b. RoboCat with Improved Legs

Figure 2 shows the CAD model for one of the left legs of the updated RoboCat, and Figure 3 shows the 2-dof RRSSR hip joint details for one left leg (Figure 3b is the same photograph as Figure 3a, but annotated with the RRSSR parameters).

The equations, analytical solutions, and results for this paper apply equally to the left-side and right-side legs – they are identical considering sagittal plane symmetry. The examples and results given later are for the left-side hips.

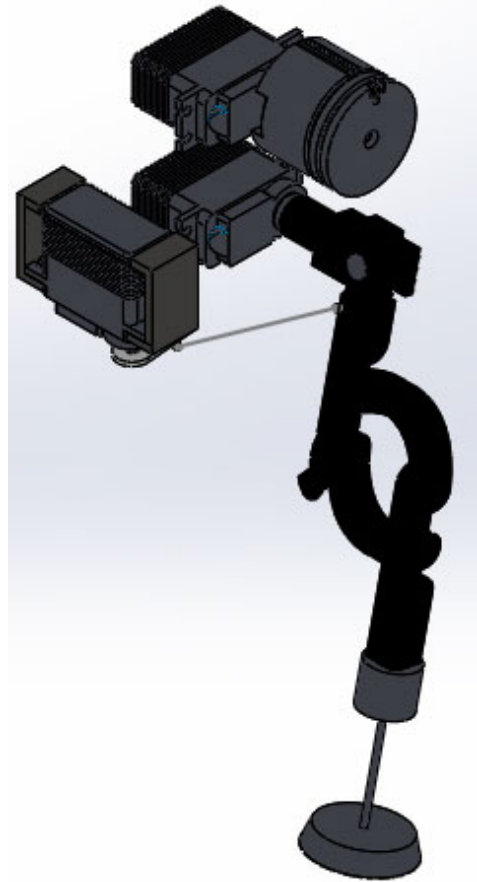


Figure 2. RoboCat Left Leg CAD Model



Figure 3a. RRSSR Left Hip

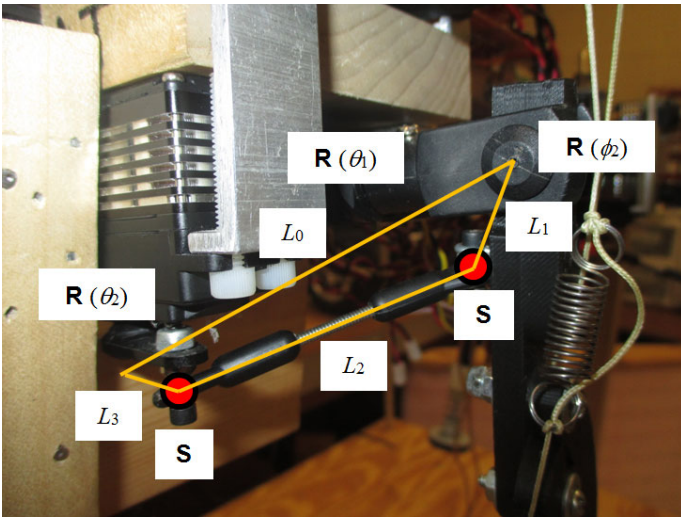


Figure 3b. RRSSR Left Hip, Annotated

The kinematics diagram for either of the two left-side-leg hips of the RoboCat quadruped is shown in Figure 4. This hip is a 2-dof RRSSR rigid-link parallel robot. The two active **R** joints (indicated by the underbars in the robot designation), fixed to the trunk of the walking cat, are actuated by servomotors with variables  $\theta_1$  and  $\theta_2$ , respectively. The **R** joint angle  $\phi_2$  is passive. Vector  $L_0$  is fixed to the trunk as shown, from the origin of reference frame  $\{0\}$  to the actuating plane of the second active **R** joint. Fixed lengths  $L_1$ ,  $L_2$ , and  $L_3$  connect the various joints as shown in Figure 4. Points  $P_1$  and  $P_3$  are the centers of their respective spherical (**S**) joints.

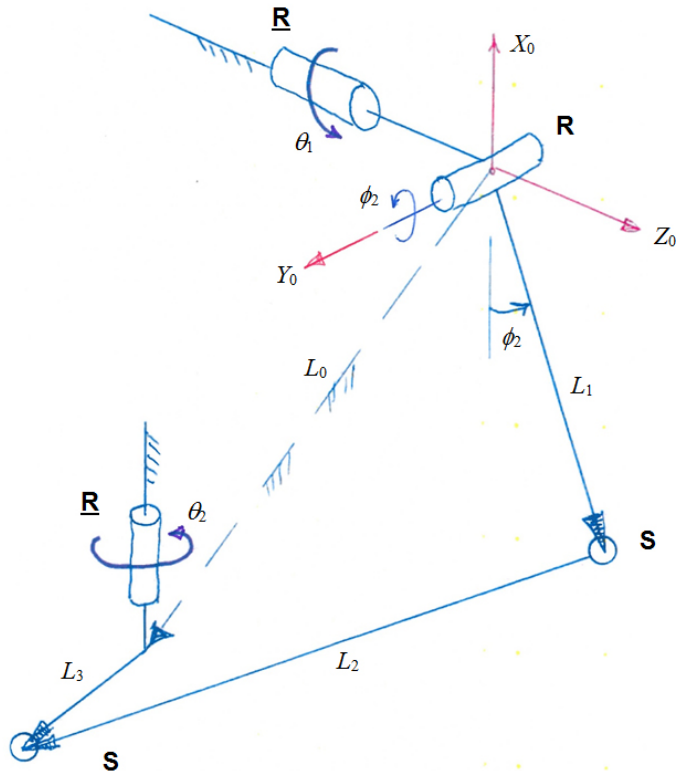


Figure 4. RRSSR Kinematic Diagram for Left Hip

The convention for zero active angle  $\theta_1$  is shown in the previous figure, i.e. with the  $\phi_2$  **R** joint axis aligned with  $Y_0$  (the  $\phi_2$  **R** joint axis rotates away from  $Y_0$  for nonzero  $\theta_1$ ). The

convention for zero passive angle  $\phi_2$  is straight down along the negative  $X_0$  axis, as shown in the previous figure. For this zero convention, the leg is not straight down, since it is inclined by constant angle  $\alpha$  due to the constant offset  $o$  (see Figure 5). Figure 5 shows a left-leg front view with  $\phi_2 = 0$ . The convention for zero active angle  $\theta_2$  is when  $L_3$  is aligned with the  $Z_0$  axis. Thus, Figure 4 shows  $\theta_2$  approaching  $-90^\circ$ . The kinematics equations and analytical solutions presented in the next section for the RRSSR parallel robot apply equally to left- and right-side legs, with proper choice of parameter constants.

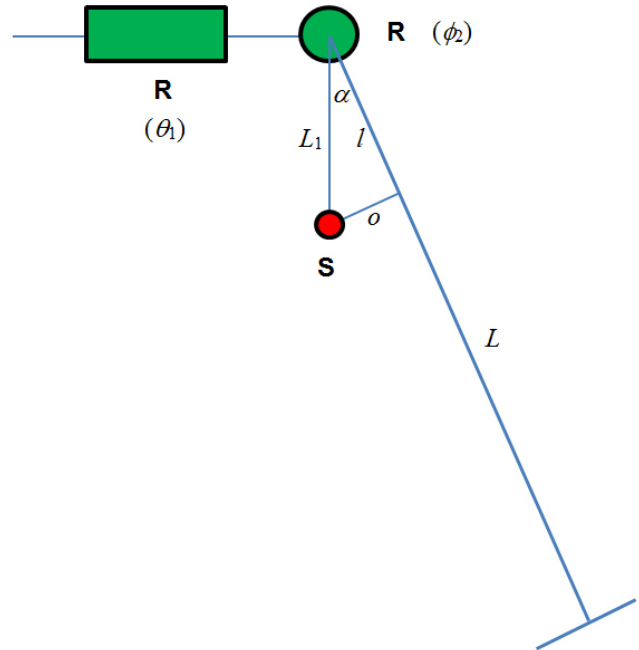


Figure 5. Left Leg Details Diagram

The RRSSR parallel robot model parameter values below are for each of the two left hips/legs of the RoboCat walking robot.

Table I. RoboCat Left Leg Parameters with Values

| name       | meaning  | value                 |
|------------|--|-----------------------|
| $L_0$      | base vector from origin to $\theta_2$ <b>R</b> joint | $[-40 \ 35 \ -65]$ mm |
| $L_1$      | <b>RS</b> length                                     | 26 mm                 |
| $L_2$      | <b>SS</b> length                                     | 55 mm                 |
| $L_3$      | <b>SR</b> length                                     | 22 mm                 |
| $o$        | perpendicular offset distance from leg to $L_1$      | 15 mm                 |
| $l$        | length along leg to $o$                              | 20 mm                 |
| $L$        | leg length   | 220 mm                |
| $\alpha$   | angle offset between $L_1$ and leg                   | $36.9^\circ$          |
| $\theta_1$ | first active joint limits                            | $\pm 90^\circ$        |
| $\theta_2$ | second active joint limits                           | $\pm 90^\circ$        |
| $\phi_2$   | passive joint limits                                 | $\pm \alpha$          |

In the RRSSR parallel robot design there are  $N = 5$  links,  $J_1 = 3$  one-dof **R** joints, and  $J_3 = 3$  three-dof **S** joints. Therefore, the spatial Kutzbach mobility equation yields:

$$\begin{aligned}
M &= 6(N-1) - 5J_1 - 4J_2 - 3J_3 - 2J_4 - 1J_5 \\
M &= 6(5-1) - 5(3) - 4(0) - 3(2) - 2(0) - 1(0) \\
M &= 24 - 15 - 6 \\
M &= 3 \quad \text{dof}
\end{aligned}$$

This mobility result is incorrect since we know that two active R joints are sufficient to control the robot, and hence  $M = 2$ . The answer to this dilemma is that there is an idle dof about the S-S link in the theoretical robot model. The hardware design locks this freedom by design and so  $M = 2$  are required.

### 3. RRSSR POSITION KINEMATICS

This section presents the position kinematics model for the 2-dof RRSSR parallel robot. The position kinematics equations are derived from a vector loop-closure equation, and then forward and inverse position kinematics equations are derived and solved analytically.

#### 3.1 Position Kinematics Equations

From the kinematic diagram of Figure 2, the following vector-loop closure equation is written for the spatial 2-dof RRSSR Robot:

$$\{\mathbf{L}_1\} + \{\mathbf{L}_2\} = \{\mathbf{L}_0\} + \{\mathbf{L}_3\}$$

where the trunk-fixed ground link vector  $\mathbf{L}_0$  and constant length  $L_0$  are:

$$\{\mathbf{L}_0\} = \begin{Bmatrix} L_{0x} \\ L_{0y} \\ L_{0z} \end{Bmatrix} \quad \text{and} \quad L_0 = \sqrt{L_{0x}^2 + L_{0y}^2 + L_{0z}^2}$$

The absolute vectors to points  $P_1$  and  $P_3$ , from the origin of the  $\{0\}$  frame and expressed in the basis of  $\{0\}$ , are:

$$\{\mathbf{P}_1\} = \{\mathbf{L}_1\} = \begin{Bmatrix} -L_1 c_1 c \phi_2 \\ -L_1 s_1 c \phi_2 \\ L_1 s \phi_2 \end{Bmatrix}$$

$$\{\mathbf{P}_3\} = \{\mathbf{L}_0\} + \{\mathbf{L}_3\} = \begin{Bmatrix} L_{0x} \\ L_{0y} - L_3 s_2 \\ L_{0z} + L_3 c_2 \end{Bmatrix}$$

where:

$$\begin{aligned}
c_1 &= \cos \theta_1 & c_2 &= \cos \theta_2 & c \phi_2 &= \cos \phi_2 \\
s_1 &= \sin \theta_1 & s_2 &= \sin \theta_2 & s \phi_2 &= \sin \phi_2
\end{aligned}$$

The kinematic constraint states that the constant length of  $L_2$  must be the vector distance between points  $P_1$  and  $P_3$ :

$$L_2 = \|\mathbf{L}_2\| = \|\mathbf{P}_3 - \mathbf{P}_1\|$$

where:

$$\{\mathbf{L}_2\} = \{\mathbf{P}_3 - \mathbf{P}_1\} = \begin{Bmatrix} L_{0x} & & + L_1 c_1 c \phi_2 \\ L_{0y} & - L_3 s_2 & + L_1 s_1 c \phi_2 \\ L_{0z} & + L_3 c_2 & - L_1 s \phi_2 \end{Bmatrix}$$

This constraint equation can be factored in two ways, one suitable for the Forward Position Kinematics (FPK) problem, and the second suitable for the Inverse Position Kinematics (IPK) problem.

#### 3.2 Forward Position Kinematics (FPK) Solutions

Forward Position Kinematics (FPK) Problem statement:

**Given:** the robot  $(\mathbf{L}_0, L_1, L_2, L_3)$ ,  $\theta_1$ , and  $\theta_2$

**Calculate:**  $\{\mathbf{P}_1\} = \begin{Bmatrix} x_1 \\ y_1 \\ z_1 \end{Bmatrix}$ ; the intermediate unknown angle  $\phi_2$  must be found first.

The kinematics constraint equation factored for the Forward Position Kinematics (FPK) problem is:

$$E_f \cos \phi_2 + F_f \sin \phi_2 + G_f = 0$$

where:

$$E_f = 2L_1(L_{0x}c_1 + s_1(L_{0y} - L_3s_2))$$

$$F_f = -2L_1(L_{0z} + L_3c_2)$$

$$G_f = L_{0x}^2 + L_{0y}^2 + L_{0z}^2 + L_1^2 - L_2^2 + L_3^2 + 2L_3(L_{0z}c_2 - L_{0y}s_2)$$

The equation form  $E_f \cos \phi_2 + F_f \sin \phi_2 + G_f = 0$  appears a lot in robot and mechanism kinematics and is readily solved using the **Tangent Half-Angle Substitution**.

$$\text{If we define} \quad t_f = \tan\left(\frac{\phi_2}{2}\right)$$

$$\text{then} \quad \cos \phi_2 = \frac{1 - t_f^2}{1 + t_f^2} \quad \text{and} \quad \sin \phi_2 = \frac{2t_f}{1 + t_f^2}$$

and the solution is:

$$t_{f,2} = \frac{-F_f \pm \sqrt{E_f^2 + F_f^2 - G_f^2}}{G_f - E_f} \quad \phi_{2,2} = 2 \tan^{-1}(t_{f,2})$$

Two  $\phi_2$  solutions result, from the  $\pm$  in the quadratic formula. For the specific RoboCat walking robot left hip/leg, only the positive sign is admissible, i.e. only  $\phi_{2,1}$  is allowed. The negative branch solution  $\phi_{2,2}$  always leads to a solution that is out of the practical workspace of the RoboCat leg, usually with

a  $+x_1$  which is impossible. Another invalid case associated with  $\phi_2$  leads to  $-x_1$ , but a violation of the  $\alpha$  angle joint limits.

The overall solution is then found from:

$$\{\mathbf{P}_1\} = \begin{Bmatrix} x_1 \\ y_1 \\ z_1 \end{Bmatrix} = \begin{Bmatrix} -L_1 c_1 c \phi_2 \\ -L_1 s_1 c \phi_2 \\ L_1 s \phi_2 \end{Bmatrix}$$

### 3.3 Inverse Position Kinematics Solutions

Inverse Position Kinematics (IPK) Problem statement:

**Given:** the robot ( $\mathbf{L}_0, L_1, L_2, L_3$ ), and

$$\{\mathbf{P}_1\} = \begin{Bmatrix} x_1 \\ y_1 \\ \pm \sqrt{L_1^2 - x_1^2 - y_1^2} \end{Bmatrix}$$

**Calculate:**  $\theta_1$  and  $\theta_2$ ; again, the intermediate unknown angle  $\phi_2$  must be found first

As shown in the given  $\{\mathbf{P}_1\}$  above, there is a constraint  $z_1 = \pm \sqrt{L_1^2 - x_1^2 - y_1^2}$  since vector  $\{\mathbf{P}_1\}$  must lie on the surface of a sphere of radius  $L_1$  centered about the  $\{0\}$  origin. Choosing only the positive value for  $z_1$  will normally result in best results for the RoboCat walking robot (left hip/leg) since that will ensure the solutions do not lie under the robot but rather with the hips generally turned out from the body in the correct direction.

Using:

$$\{\mathbf{P}_1\} = \{\mathbf{L}_1\} = \begin{Bmatrix} -L_1 c_1 c \phi_2 \\ -L_1 s_1 c \phi_2 \\ L_1 s \phi_2 \end{Bmatrix}$$

that was presented before, we can first solve for unknown intermediate angle  $\phi_2$ :

$$\phi_{2,1,2} = \text{atan2}(z_1, \pm \sqrt{x_1^2 + y_1^2})$$

To ensure that the resulting angle  $\phi_2$  lies within the practical robot joint limits, only  $\phi_2$  (the positive solution branch) should be used. After solving  $\phi_2$ , the single correct value for  $\theta_1$  is found from:

$$\theta_1 = \text{atan2} \left[ \frac{-y_1}{c \phi_2}, \frac{-x_1}{c \phi_2} \right]$$

Though the magnitude of  $c \phi_2$  cancels out in the calculation of  $\theta_1$ , it still must be included to ensure the atan2 function selects the correct quadrant for angle  $\theta_1$ .

Given values for both angles  $\theta_1$  and  $\phi_2$ , we find the remaining unknown angle  $\theta_2$  using a different factoring of the original constraint equation.

The kinematics constraint equation factored for the Inverse Position Kinematics (IPK) problem is:

$$E_i \cos \theta_2 + F_i \sin \theta_2 + G_i = 0$$

where:

$$\begin{aligned} E_i &= 2L_3(L_{0z} - L_1 s \phi_2) \\ F_i &= -2L_3(L_{0y} + L_1 s_1 c \phi_2) \\ G_i &= L_{0x}^2 + L_{0y}^2 + L_{0z}^2 + L_1^2 - L_2^2 + L_3^2 \\ &\quad + 2L_1((L_{0x} c_1 + L_{0y} s_1) c \phi_2 - L_{0z} s \phi_2) \end{aligned}$$

Again, this equation can be solved using the **Tangent Half-Angle Substitution**.

$$t_i = \tan \left( \frac{\theta_2}{2} \right)$$

$$t_{i,2} = \frac{-F_i \pm \sqrt{E_i^2 + F_i^2 - G_i^2}}{G_i - E_i} \quad \theta_{2,1,2} = 2 \tan^{-1}(t_{i,2})$$

Two  $\theta_2$  solutions result, from the  $\pm$  in the quadratic formula. In general both  $\theta_2$  solutions yield valid solution branches, when combined with the one valid  $\theta_1$  from above. For the specific RoboCat walking robot, the negative branch, i.e.  $\theta_2$ , is recommended. This will ensure a control variable  $\theta_2$  closer to the midrange nominal value  $\theta_2 = 0$ . This is because the  $\theta_2$  **R** joint is positioned forward of the  $\theta_1$  **R** joint on the left side of this robot. Hence the opposite solution should be chosen for the right side of the walking robot.

## 4. RESULTS

### 4.1 MATLAB Circular Check Examples

MATLAB Software was used to implement the analytical solutions for the RRSSR parallel robot forward and inverse position kinematics equations. The various multiple solutions and how to choose the preferred solutions were included. A large number of simple and then complicated examples were tested, and all proved to be valid using the circular check between the forward and inverse position kinematics MATLAB programs. That is, for all examples (not shown), the output of the FPK program was used as input to the IPK program and the correct results were generated. Also, the output of the IPK

program was used as input to the FPK program and the correct results were again generated.

#### 4.2 RoboCat Hardware Measurements

Three position examples were generated using the FPK and IPK MATLAB programs discussed above. The same position examples were used with the RoboCat hardware of Figures 1 and 3. The position kinematics results were measured physically with digital calipers for distance and a protractor for angular results. These hardware values were then compared to the MATLAB model results (see the following subsection).

#### 4.3 MATLAB/Hardware Results Validation

This subsection presents three examples comparing the MATLAB FPK and IPK simulation results vs. physical measurement of the hardware positions for the same RRSSR parallel robot dimensions (Table I) and input parameters. The  $x, y, z$  data reported in the three tables below are the  $\{0\}$  frame components of vector  $\{P_1\}$ . Angles  $\theta_1, \theta_2,$  and  $\phi_2$  refer to those of the robot model identified in Figure 4; angular limits for these angles are given in Table I.

Tables IIa, IIb, and IIc present this comparison between MATLAB model and hardware measurement results. The associated graphical results (MATLAB and hardware photograph) are given in Figures 6a, 6b, and 6c, respectively. The first two examples stemmed from FPK and the third example started with IPK. As seen in the data of the tables below, the agreement is quite good considering relatively low precision (especially for the angular measurements) in measurements of the hardware.

**Table IIa. Example 1 Validation Results (degrees for angles, mm for length)**

|          | $\theta_1$ | $\theta_2$ | $\phi_2$ | $x$   | $y$ | $z$  |
|----------|------------|------------|----------|-------|-----|------|
| MATLAB   | 0          | 0          | -4.3     | -26.6 | 0   | -2.0 |
| Hardware | 0          | 0          | -7       | -24.6 | 0   | -3.9 |

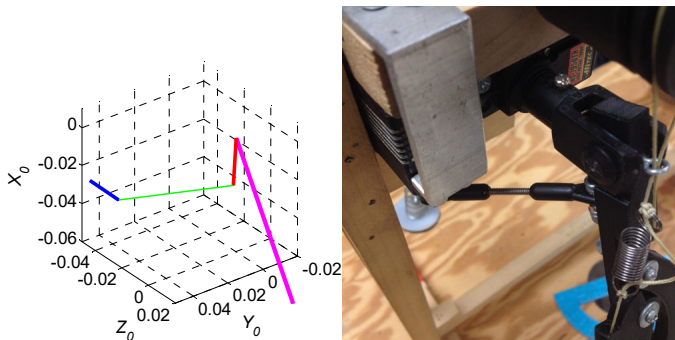


**Figure 6a. Ex 1 MATLAB Model and Photograph**

**Table IIb. Example 2 Validation Results (degrees for angles, mm for length)**

|        | $\theta_1$ | $\theta_2$ | $\phi_2$ | $x$   | $y$ | $z$  |
|--------|------------|------------|----------|-------|-----|------|
| MATLAB | 0          | 90         | -32.2    | -22.2 | 0   | -1.4 |

| Hardware | 0 | 90 | -26 | -23.4 | 0 | -1.5 |
|----------|---|----|-----|-------|---|------|
|----------|---|----|-----|-------|---|------|

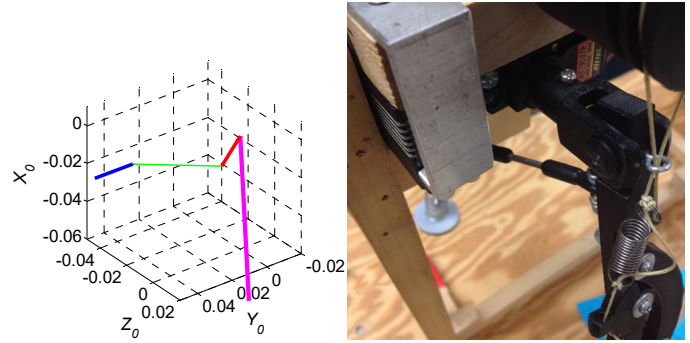


**Figure 6b. Ex 2 MATLAB Model and Photograph**

**Table IIc. Example 3 Validation Results (degrees for angles, mm for length)**

|          | $\theta_1$ | $\theta_2$ | $\phi_2$ | $x$   | $y$ | $z$  |
|----------|------------|------------|----------|-------|-----|------|
| MATLAB   | -15.0      | 78.0       | -16.9    | -24.3 | 6.5 | -7.6 |
| Hardware | -15.0      | 78.0       | -20      | -20.9 | 3.2 | -7.8 |

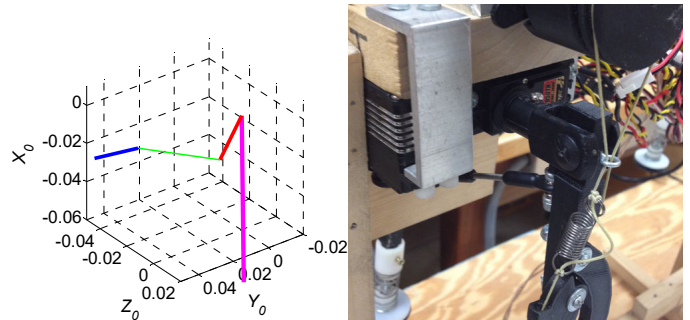


**Figure 6c. Ex 3 MATLAB Model and Photograph**

Upon inspection of the data we can see that there is a good similarity between the MATLAB and hardware data sets. Data for positions one and two exhibit the most similarity to the results in MATLAB; position three exhibits more error than the other two positions. Since this is a more general position that was more difficult to measure, the error can be attributed to human error during measurement. Error in all position data can also be attributed to some play in the hardware. The precision of this data was not meant to be great. Its purpose is to simply demonstrate the feasibility of using both forward and inverse position MATLAB models on the 2-DOF RRSSR robot hardware.

#### 4.4 RRSSR Parallel Robot Workspace

Let us define the RRSSR parallel robot workspace as the locus of points reachable by the passive **S** joint point  $\{P_1\}$ . Then this 2-dof robot workspace is limited to the surface of a sphere, reduced by the applicable joint limits given in Table I. Figure 7 shows the reachable workspace for the RoboCat left hip. The right hip workspace is symmetric to this result.

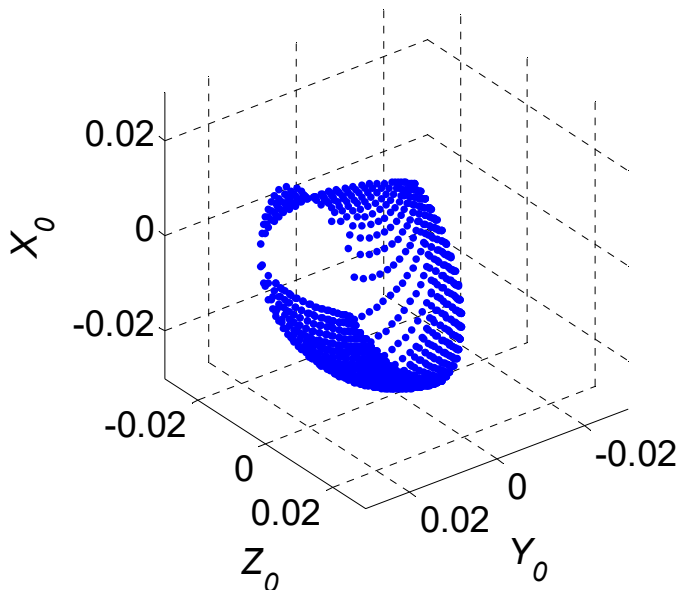


Figure 7. RRSSR Left Hip Reachable Workspace

## 5. CONCLUSION

This paper has presented forward and inverse position kinematics equations and analytical solutions for the 2-dof RRSSR Parallel Robot, including how to select amongst the multiple solutions in each case. This rigid-link parallel robot serves as the hip joints of the Ohio University RoboCat walking quadruped. The methods of this paper can be used for quadruped design, simulation, control, and gait selection. The RoboCat hardware was used to validate the MATLAB examples for the analytical solutions of this paper. Subject to limitations in measurement precision, the three examples were validated. This paper does not introduce any new techniques; instead, its contribution is the analytical solutions for the forward and inverse position kinematics of the RRSSR Parallel Robot, which have not been previously presented.

## ACKNOWLEDGEMENTS

We would like to thank Brian Berthold, Ohio University undergraduate research assistant, for the CAD drawing.

## REFERENCES

- [1] R.L. Williams II, 1985, "Computer-Aided Synthesis and Analysis of Spatial RSSR Mechanisms", MS Thesis, Department of Mechanical Engineering, Virginia Polytechnic Institute and State University, Blacksburg, VA, August.
- [2] B.W. Mooring, Z.S. Roth, and M.R. Driels, 1991, Fundamentals of Manipulator Calibration, John Wiley & Sons, Inc., New York, NY.
- [3] P.A. Simionescu, I. Tempea, and N.E. Loch, 2001, "Kinematic analysis of a two-degree-of-freedom steering mechanism used in rigid-axle vehicles", Proceedings of the Institution of Mechanical Engineers, Part D, Journal of Automobile Engineering, 215(7):803-812, DOI: 10.1243/0954407011528392.
- [4] P.A. Simionescu and M.R. Smith, 2000, "Single-valued function representations in linkage mechanisms design", Mechanism and Machine Theory, 35(12):1709-1726. DOI: 10.1016/S0094-114X(00)00018-5.
- [5] P.A. Simionescu, D. Beale, and I. Talpasanu, 2007, "Dynamic effect of the bump steer in a wheeled tractor", Mechanism and Machine Theory, 42(10):1352-1361, DOI: 10.1016/j.mechmachtheory.2006.10.007.
- [6] S. Li and J.S. Dai, 2012, "Structure Synthesis of Single-Driven Metamorphic Mechanisms Based on the Augmented Assur Groups", ASME Journal of Mechanisms and Robotics, 4(3): 031004, 8 pages, DOI 10.1115/1.4006741.